Russian Physics Journal, Vol. 53, No. 3, 2010

TRANSLATIONALLY INVARIANT KINK SOLUTIONS OF DISCRETE ϕ^4 MODELS

J. A. Baimova,[1] Yu. V. Bebikhov,[2] S. V. Dmitriev,[1] A. Khare,[3] and A. I. Potekaev[4]

UDC 539.2

The properties of translationally invariant kinks in two discrete ϕ^4 models are compared with those of the kinks in a classical discrete model. The translationally invariant kink solutions can be found randomly with respect to the lattice sites, i.e., their Peierls–Nabarro potential is exactly equal to zero. It is shown that these solutions have a Goldstone mode, that is, they can move along the lattice at vanishingly small velocities. Thus, the translationally invariant kink is not trapped by the lattice and can be accelerated by an arbitrary small external field and, having an increased mobility, can transfer a range of physical quantities: matter, energy, momentum, etc.

Keywords: discrete models, translationally invariant structures.

INTRODUCTION

Discrete models for the Klein–Gordon equation, which admit exact translationally invariant (TI) static solutions (i.e., solutions containing an arbitrary displacement along the lattice, x_0), were constructed and investigated by a large number of authors [1–17]. To begin with, we would like to note that here we mean nonintegrable chains (such as the Toda chain) [18]). Nonintegrable discrete equations admitting exact TI static solutions will be here referred to as TI discrete equations; though in a strict mathematical meaning they do not possess this property. The theory of TI discrete equations is closely connected with the theory of integrable maps [2–4]. In [2] it is proposed to treat integrable maps as a new class of integrable equations. This work also describes a family of the second-order integrable difference equations and their first integrals and establishes the relation between the maps and the Jacobi elliptic functions.

The approach to discretization of the Klein–Gordon equation proposed by Speight and Ward [5] and Speight [6, 7] is based on implementing the Bogomol'nyi idea [19] to discrete equations. They demonstrated that kink solutions for the discrete models thus derived could be found from a two-point map.

The approach to discretization of the Klein–Gordon equation used by Kevrekidis [8] yielded a class of models whose exact static TI solutions are found from an integrable map.

A different approach to finding solutions to discrete equations admitting TI static solutions relies on the use of the discretized first integral (DFI) of the initial continuous equation taken in a static form [9]. The DFI method was developed in [10] and today is the most general approach to constructing TI-discretizations of the second-order nonlinear equations.

Translationally invariant static solutions possess the following properties: 1) there is no any Peierls–Nabarro energy relief, i.e., there are no energy barriers between the static solutions with different positions with respect to the lattice x_0, 2) static TI solutions could be found by iteration from two-point maps, and 3) static TI solutions contain a Goldstone (translational) mode for any x_0.

---

[1]Institute for Metals Superplasticity Problems of the Russian Academy of Sciences, Ufa, Russia, e-mail: dmitriev.sergey.v@gmail.com, [2]I. I. Polzunov Altai State Technical University, Barnaul, Russia, [3]Institute of Physics, Bhubaneshwar, India, [4]V. D. Kuznetsov Siberian Physical-Technical Institute at Tomsk State University, Tomsk, Russia. Translated from Izvestiya Vysshikh Uchebnykh Zavedenii, Fizika, No. 3, pp. 20–25, March, 2010. Original article submitted September 30, 2009.

Thus we can argue that TI static solutions (e.g., soliton TI solutions) are not trapped by the lattice and can be accelerated by an arbitrary weak external field. This property makes the models admitting such solutions potentially useful for applications; one such physical model has been recently proposed in [16]. There is a good reason to assume that the number of systems described without the Peierls–Nabarro potential (or with a very low Peierls–Nabarro barrier) would grow, and these models would find their due place in modern natural science.

It was shown for certain Klein–Gordon TI models that they conserve momentum [8, 14] and energy (Hamiltonian) [5–7, 11, 13]. However, we are not aware of any Klein–Gordon TI model conserving both the momentum and energy. Moreover, for a momentum defined in a conventional manner it was proved that its conservation rules out a possibility of energy conservation [12].

Despite the fact that the number of well-known discrete equations admitting TI static solutions is quite large, their properties are still weakly investigated. In this work we are going to discuss kink TI solutions for two such models, and their properties will be compared to those of the kinks in a classical discrete ϕ^4 model.

1. THREE DISCRETE ϕ^4 MODELS

A continuous ϕ^4 equation is given by

$$\phi_{tt} = \phi_{xx} + 2\phi\left(1-\phi^2\right), \tag{1}$$

and the first integral of its static version is

$$U(x) \equiv \phi_x^2 - \left(1-\phi^2\right)^2 = 0, \tag{2}$$

where we take the integration constant to be zero, which corresponds to the kink solutions in [10]. The first integral will be also considered in a modified form

$$u(x) \equiv \pm\phi_x - 1 + \phi^2 = 0. \tag{3}$$

Let us describe three different discretizations of equation (1) and then compare the properties of their kink solutions. We introduce a notation for the linear difference operator

$$\Delta_2\phi_n = \frac{1}{h^2}(\phi_{n-1} - 2\phi_n + \phi_{n+1}). \tag{4}$$

Model 1. A classical model with the Peierls–Nabarro potential is given by

$$\ddot{\phi}_n = \Delta_2\phi_n + 2\phi_n\left(1-\phi_n^2\right) \tag{5}$$

and it conserves total energy

$$H_1 = \frac{h}{2}\sum_n\left[\dot{\phi}_n^2 + \frac{1}{h^2}(\phi_n - \phi_{n-1})^2 + \left(1-\phi_n^2\right)^2\right]. \tag{6}$$

Static kinks for this model exist only in the case of their centering on the chain site (steady state corresponding to the Peierls–Nabarro potential minimum) or in the middle between the two nearest sites (unstable state corresponding to the Peierls–Nabarro potential maximum). Exact solutions for the static kinks are unknown. The following approximated solution could be taken as a first approximation:

$$\phi_n = \pm\tanh\left[h(n-x_0)\right]. \tag{7}$$

Consider a small perturbation of an equilibrium solution ϕ_n^0 given by $\phi_n(t)=\phi_n^0+\varepsilon_n(t)$, and derive a linearized equation for the perturbation

$$\ddot{\varepsilon}_n = \Delta_2\varepsilon_n - 6\left(\phi_n^0\right)^2\varepsilon_n. \tag{8}$$

For the low-amplitude phonons $\varepsilon_n = \exp(ikn - i\omega t)$, where ω is the frequency and k is the wave number. From (8), let us derive the following dispersion relation:

$$\omega^2 = \frac{4}{h^2}\sin^2\left(\frac{k}{2}\right) - 2 + 6\left(\phi_n^0\right)^2, \tag{9}$$

and from (9) – the vacuum spectrum $\phi_n^0 = \pm 1$

$$\omega^2 = 4 + \frac{4}{h^2}\sin^2\left(\frac{k}{2}\right). \tag{10}$$

Model 2. Speight–Ward Model [5–7].

Let us consider a DFI obtained via discretization of equation (3):

$$u_2 \equiv \pm\frac{1}{h}(\phi_n - \phi_{n-1}) - 1 + \frac{1}{3}\left(\phi_{n-1}^2 + \phi_{n-1}\phi_n + \phi_n^2\right) = 0\,. \tag{11}$$

A Hamiltonian given by

$$H_2 = h\sum_n\left(\frac{\dot{\phi}_n^2}{2} + u_2^2\right) \tag{12}$$

yields the equations of motion

$$\begin{aligned}\ddot{\phi}_n &= -u_2(\phi_{n-1},\phi_n)\frac{\partial}{\partial\phi_n}u_2(\phi_{n-1},\phi_n) - u_2(\phi_n,\phi_{n+1})\frac{\partial}{\partial\phi_n}u_2(\phi_n,\phi_{n+1}) \\ &= \left(1+\frac{h^2}{3}\right)\Delta_2\phi_n + 2\phi_n - \frac{1}{9}\left[2\phi_n^3 + (\phi_{n-1}+\phi_n)^3 + (\phi_n+\phi_{n+1})^3\right].\end{aligned} \tag{13}$$

It is evident that the static solutions to the model (13) can be found from a two-point difference equation (11), which can be re-written as a nonlinear map as follows:

$$\phi_{n\pm1} = -\frac{\phi_n}{2} \mp \frac{3}{2h} \pm \frac{\sqrt{3}}{2}\sqrt{-\phi_n^2 \pm \frac{6}{h}\phi_n + \frac{3}{h^2} + 4}\,, \tag{14}$$

where one can take either the upper or the lower signs. A kink solution can be found via iterating Eq. (14). In so doing, for a kink centered on the lattice node one should take $\phi_0 = 0$, while for the one centered in between the nodes – $\phi_0 = 3/h - \sqrt{3+9/h^2}$.

Equation (13), linearized in the vicinity of a static solution ϕ_n^0, is given by

$$\ddot{\varepsilon}_n = \left(1+\frac{h^2}{3}\right)\Delta_2\varepsilon_n + 2\varepsilon_n - \frac{1}{9}\left[6\left(\phi_n^0\right)^2\varepsilon_n + 3\left(\phi_n^0+\phi_{n-1}^0\right)^2(\varepsilon_n+\varepsilon_{n-1}) + 3\left(\phi_n^0+\phi_{n+1}^0\right)^2(\varepsilon_n+\varepsilon_{n+1})\right]. \quad (15)$$

The vacuum spectrum, $\phi_n^0 = \pm 1$, has the following form:

$$\omega^2 = 4 + 4\frac{1-h^2}{h^2}\sin^2\left(\frac{k}{2}\right). \quad (16)$$

Model 3. This model was discussed in, e.g., [11, 13].
Let us consider a DFI derived by discretization of equation (2):

$$U_3 \equiv \frac{1}{h^2}(\phi_n - \phi_{n-1})^2 - (1-\phi_{n-1}\phi_n)^2 = 0. \quad (17)$$

The equations of motion for Model 3

$$\ddot{\phi}_n = \frac{U_3(\phi_n,\phi_{n+1}) - U_3(\phi_{n-1},\phi_n)}{(\phi_{n+1}-\phi_{n-1})\left(1-h^2\phi_n^2\right)} = \Delta_2\phi_n + 2\frac{\phi_n - \phi_n^3}{1-h^2\phi_n^2} \quad (18)$$

are found from the Hamiltonian

$$H_3 = \frac{1}{2}\sum_n\left(\frac{\dot{\phi}_n^2}{2} + \frac{(\phi_n-\phi_{n-1})^2}{h^2} + V(\phi_n)\right),$$
$$V(\phi_n) = -\frac{1}{h^2}\left(\phi_n^2 + \frac{1-h^2}{h^2}\ln\left|\phi_n^2 - \frac{1}{h^2}\right|\right). \quad (19)$$

It is evident that the static solutions to the model (18) can be found from a two-point problem (17), which could be written as a map given by

$$\phi_n = \frac{\phi_{n-1} \pm h}{1 \pm h\phi_{n-1}}, \quad (20)$$

where we can take either upper or the lower signs and swap the positions of ϕ_n and ϕ_{n-1}. As an initial value for a kink centered on the lattice site one should take $\phi_0 = 0$, and for the one centered in between the sites – $\phi_0 = 1/h - \sqrt{1/h^2 - 1}$. The model also admits a kink solution in an explicit form

$$\phi_n = \pm\tanh[\beta h(n-x_0)], \qquad \tanh(\beta h) = h, \quad (21)$$

where x_0 is an arbitrary displacement.

Equation (18), linearized in the vicinity of a static solution ϕ_n^0, is given by

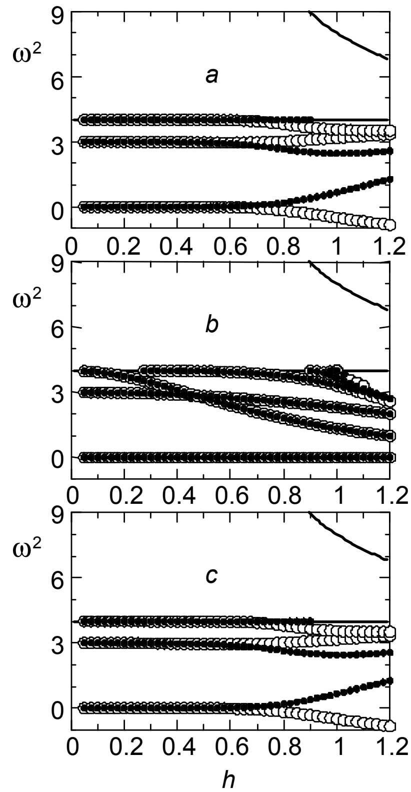

Fig. 1. Vibrational spectrum from a chain containing a kink for three models: Model 1 (*a*), Model 2 (*b*), and Model 3 (*c*). Full lines show the phonon spectrum boundaries of a chain without a kink, and circles (full circles) – frequencies of the vibrational modes localized on a kink centered on a site (or between the nearest sites).

$$\ddot{\varepsilon}_n = \Delta_2 \varepsilon_n + 2\frac{1+\left(h^2-3\right)\left(\phi_n^0\right)^2 + h^2\left(\phi_n^0\right)^4}{\left[1-h^2\left(\phi_n^0\right)^2\right]^2}\varepsilon_n . \tag{22}$$

The vacuum spectrum $\phi_n^0 = \pm 1$ has the following form:

$$\omega^2 = \frac{4}{1-h^2} + \frac{4}{h^2}\sin^2\left(\frac{k}{2}\right). \tag{23}$$

2. VIBRATIONAL KINK SPECTRA

Let us compare the vibrational spectra of the kinks in three discrete ϕ^4 models and vacuum spectra in these models. The results are presented in Fig. 1. The boundaries of the phonon vacuum spectrum are depicted by full lines, and open and full circles show the frequencies of the vibrational modes localized on a kink centered on a site $(x_0 = 0)$ and in the middle between the nearest sites $(x_0 = 1/2)$, respectively. The spectra were calculated for a chain of $N = 200$ particles with a kink in the middle for the case of anti-periodic boundary conditions.

All the three models in a continuous limit $(h \to 0)$ are reduced to one and the same equation (1). Their properties are, therefore, close at small values of h, and so are their spectra; this is evident from a comparison in Fig. 1. One can see that as h increases the difference between the spectra for different models also increases.

Attention should be primarily paid to the principal differences of the spectrum of Model 1, having a Peierls–Nabarro potential, from those of Models 2 and 3 without this potential. Models 2 and 3 for any h and any kink position with respect to the lattice x_0 have a zero-frequency mode. This is a Goldstone (translational) mode reflecting a latent symmetry of Models 2 and 3. In Model 1, this mode exists only for small values of h, i.e., it is inherited from the continuous model but disappears as the system becomes more discrete. The difference in the behavior of this mode for the kinks with $x_0 = 0$ and 1/2 (Fig. 1*a*) is also significant. In the first case, with increase in h the squared frequency is increased, while in the second case it decreases and acquires negative values, which testifies to the instability of an equilibrium kink centered on a lattice site. The kinks shown in Fig.1*a* and *b* are in the state of indifferent stable equilibrium for any x_0.

There are some other spectrum differences not associated with the presence or absence of translation invariance. Let us describe them, starting from the vacuum spectra and then for the kink spectra. In Model 1, the vacuum spectral width turns to zero only for $h \to 0$ (recall that the vacuum spectrum boundaries are shown by full lines in Fig. 1). Vacuum in this model is set to be always stable, since $\omega^2 > 0$ for any h. In Model 2, the vacuum spectral width vanishes at $h = 1$. Vacuum in this model is always stable, since $\omega^2 > 0$ for any h. Model 3 has a cubic term depending on h. The lower boundary of the vacuum spectrum is therefore dependent on h, while in the other models it is constant $\left(\omega^2 = 4\right)$. Vacuum is stable only for $0 < h < 1$.

Let us now compare frequencies of the modes localized on the kink. For small values of $h(< 0,4)$ and even for not too small values $h(< 0.8)$ all three models have a translational mode and two localized modes lying beyond the vacuum spectrum. One of them is very close to the lower boundary of the phonon spectrum $\left(\omega^2 = 4\right)$, and the second is located at $\omega^2 \approx 3$, which corresponds to a well-known vibrational kink mode in the continuous ϕ^4 equation. For large values of h, other localized modes are found in the kink spectrum.

3. KINK MOBILITY

Shown in Fig. 2 are the numerical results on kink velocity variation within a comparatively long time period for different initial kink velocities. Two discrete models are compared: classical discretization, Model 1 (*a*) with a Peierls–Nabarro potential and Model 2 with TI static kinks.

It is evident from Fig. 2*a* that in the classical model the kink moves without any noticeable loss of its velocity only at velocities lower than 0.2. At larger velocities, the kink radiates energy very fast and loses the kinetic energy of motion. In Model 2, the kinks virtually do not radiate energy, moving at much higher velocities up to 0.5. This evidences of much higher kink mobility in Model 2 compared to the classical model.

SUMMARY

In this work we have compared physical properties of three discrete ϕ^4 models: classical discretization and two other discretizations admitting static TI kinks. In [21–23] we investigated the behavior of the simplest topological soliton, in particular, a kink. Here we have compared vibrational spectra of chains involving a single static kink. In addition, we have investigated kink mobility in TI models in comparison with the classical model.

It has been shown that the properties of three discrete models differ but slightly at low values of h, which is accounted for by the fact that in a continuous limit all three models are reduced to a continuous ϕ^4 equation. With an increase in h the properties of discrete models begin to show pronounced differences from those of a continuous equation and differ between each other.

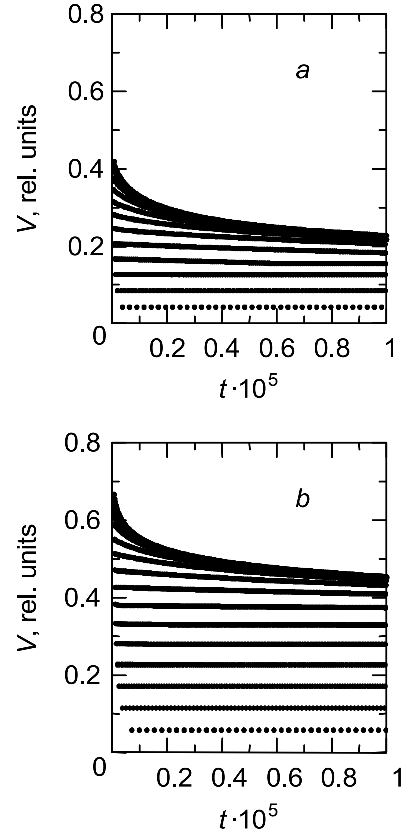

Fig. 2. Kink velocity variation in time for different initial velocities. A comparison of two discrete models: classical discretization, Model 1 with a Peierls–Nabarro potential (*a*) and TI model with total energy conservation (*b*). The result is given for $h = 0.7$.

In the models ensuring the existence of a static TI kink solution, there is a zero-frequency translational Goldstone mode in the vibrational kink spectrum. This statement is valid for a static kink located arbitrarily with respect to the lattice. In the classical model, the kinks exist only in two high-symmetry configurations. For one of them, in particular, a kink centered on a lattice site, the analog of a Goldstone mode has an imaginary frequency, which is indicative of unstable kink equilibrium in this position with respect to the lattice. For a kink centered in the middle between two nearest sites, the analog of a Goldstone mode has a non-zero positive velocity, which is indicative of the presence of a Peierls–Nabarro potential in the classical model. In the models with TI kinks this potential is absent, the kinks in their potential relief are not associated with the lattice, can move along it at a low velocity, and can be accelerated by an arbitrarily low external field. Even at considerably high velocities of motion, when kinks begin to radiate energy, they are frequently more mobile than in the classical discrete model. Radiation from a kink moving at a finite velocity in TI models is associated with the fact that these models are nonintegrable in a dynamic formulation, though these models are integrable in a static formulation, when described by integrable maps.

It is well known that topological solitons, such as kinks, can, depending on applications, transfer mass, energy, momentum, electrical discharge, data, etc. Based on the results of this work, we can draw a conclusion on advanced transport properties of discrete models admitting static TI kink solutions.

This work was supported by the RFBR grants, Nos. 08-02-91316-ИНД_a and 09-08-00695-a, and a Povolzhye grant from the Bashkortostan Academy of Sciences No. 40/61-П.

REFERENCES

1. C. M. Bender and A. Tovbis, J. Math. Phys., **38**, 3700 (1997).
2. G. R. W. Quispel, J. A. G. Roberts and C. J. Thompson, Physica D, 34, 183 (1989).
3. R. Hirota, K. Kimura, and H. Yahagi, J. Phys. A, **34**, 10377 (2001).
4. N. Joshi, B. Grammaticos, T. Tamizhmani, *et al*., Lett. Math. Phys., **78**, 27 (2006).
5. J. M. Speight and R. S. Ward, Nonlinearity, **7**, 475 (1994).
6. J. M. Speight, *Ibid*., **10**, 1615 (1997).
7. J. M. Speight, *Ibid*., **12**, 1373 (1999).
8. P. G. Kevrekidis, Physica D, **183**, 68 (2003).
9. S. V. Dmitriev, P. G. Kevrekidis, and N. Yoshikawa, J. Phys. A: Math. Gen., **38**, 7617 (2005).
10. I. V. Barashenkov, O. F. Oxtoby, and D. E. Pelinovsky, Phys. Rev. E, **72**, 35602R (2005).
11. F. Cooper, A. Khare, B. Mihaila, and A. Saxena, *Ibid*., **72**, 36605 (2005).
12. S. V. Dmitriev, P. G. Kevrekidis, and N. Yoshikawa, J. Phys. A: Math. Gen., **39**, 7217 (2006).
13. S. V. Dmitriev, P. G. Kevrekidis, N. Yoshikawa, *et al*., Phys. Rev. E, **74**, 046609 (2006).
14. S. V. Dmitriev, P. G. Kevrekidis, A. Khare *et al*., J. Phys. A: Math. Theor., **40**, 6267 (2007).
15. I. Roy, S. V. Dmitriev, P. G. Kevrekidis, *et al*., Phys. Rev. E, **76**, 026601 (2007).
16. J. M. Speight and Y. Zolotaryuk, Nonlinearity, **19**, 1365 (2006).
17. S. V. Dmitriev, A. Khare, P. G. Kevrekidis, *et al*., Phys. Rev. E, **77**, 056603 (2008).
18. M. Toda, J. Phys. Soc. Jpn. , **22**, 431 (1967).
19. E. V. Bogomol'nyi, J. Nucl. Phys., **24**, 449 (1976).
20. T. I. Belova and A. E. Kudryavtsev, Uspekhi Fiz. Nauk, **167**, 377 (1997).
21. S. V. Dmitriev, N. N. Medvedev, R. R. Mulukov, *et al*., Rus. Phys. J., V. 51, No. 8, 858–865 (2008).
22. S. V. Dmitriev, A. A. Nazarov, A. I. Potekaev, *et al*., *Ibid*., No. 2, 132–137 (2009).
23. S. V. Dmitriev, A. I. Potekaev, and A. V. Samsonov, *Ibid*., V. 52, No. 6, 622–639 (2009).